CONSTRAINED MULTI-OBJECTIVE OPTIMIZATION OF HELIUM LIQUEFACTION CYCLE

Min SHI [1,2], Tongqiang SHI [4], Lei SHI [1], Zhengrong OUYANG [3], Junjie LI [1,2*]

[1]High Magnetic Field Laboratory, HFIPS, Anhui, Chinese Academy of Sciences, Hefei 230031, China

[2]University of Science and Technology of China, Hefei 230026, China

[3]School of Physical Science and Technology, Shanghai Tech University, Shanghai 201210, China

[4]Anhui Wanrui Cold Power Technology Co., Ltd., Hefei 230088, China

[*] Corresponding author; E-mail: shimin@mail.ustc.edu.cn

The helium cryo-plant is an indispensable subsystem for the application of low-temperature superconductors in large-scale scientific facilities. However, it is important to note that the cryo-plant requires stable operation and consumes a substantial amount of electrical power for its operation. Additionally, the construction of the cryo-plant incurs significant economic costs. To achieve the necessary cooling capacity while reducing power consumption and ensuring stability and economic feasibility, constrained multi-objective optimization is performed using the interior point method in this work. The Collins cycle, which uses liquid nitrogen precooling, is selected as the representative helium liquefaction cycle for optimization. The discharge pressure of the compressor, flow ratio of turbines, and effectiveness of heat exchangers are taken as decision parameters. Two objective parameters, cycle exergy efficiency ($\eta_{\mathrm{Ex,cycle}}$) and liquefaction rate ($\dot{m}_{\mathrm{L}}$), are chosen, and the wheel tip speed of turbines and UA of heat exchangers are selected as stability and economic cost constraints, respectively. The technique for Order of Preference by Similarity to the Ideal Solution (TOPSIS) is utilized to select the final optimal solution from the Pareto frontier of constrained multi-objective optimization. Compared to the constrained optimization of $\eta_{\mathrm{Ex,cycle}}$, the TOPSIS result increases the $\dot{m}_{\mathrm{L}}$ by 23.674%, but there is an 8.162% reduction in $\eta_{\mathrm{Ex,cycle}}$. Similarly, compared to the constrained optimization of $\dot{m}_{\mathrm{L}}$, the TOPSIS result increases the $\eta_{\mathrm{Ex,cycle}}$ by 57.333%, but a 10.821% reduction in $\dot{m}_{\mathrm{L}}$ is observed. This approach enables the design of helium cryo-plants with considerations for cooling capacity, exergy efficiency, economic cost, and stability. Furthermore, the wheel tip speed and UA of heat exchangers of the solutions in the Pareto frontier are also studied.

Keywords*: Collins cycle, helium cryo-plants, constrained multi-objective optimization, exergy efficiency, stability*

1. Introduction

Helium cryo-plants are indispensable subsystems in large-scale scientific facilities that rely heavily on low-temperature superconductor (LTS) magnets, such as the Spallation Neutron Source [1], Continuous Electron Beam Accelerator Facility [2], Facility for Rare Isotope Beams [3], Experimental and Advanced Superconducting Tokamak facility [4], International Thermonuclear Experimental Reactor [5], Large Hadron Collider [6], and others. These facilities demand cooling capacities ranging from thousands to tens of thousands of watts, necessitating cryogenic systems with power consumption ranging from several to tens of megawatts. Additionally, the economic cost of these cryo-plants is significant and often represents a considerable portion of the total capital expenditure of large-scale scientific projects. Furthermore, the stability of cryogenic systems needs to be a key consideration given the long-term operation of large scientific devices. Thus, it is crucial to optimize helium cryo-plants to address economic, thermodynamic, and stability considerations concurrently.

Parameter sensitivity analysis is a widely used method in single-objective optimization studies of helium liquefaction cycles. It involves assigning different values to decision parameters such as the flow ratio of turbines [7], effectiveness and UA (the product of the overall heat transfer coefficient and heat exchange area) of heat exchangers [8, 9], the discharge pressure of compressors [7, 8], the number of cooling stages [12-14] and operation modes (including pure refrigeration mode, pure liquefaction mode, and mixed mode) [15-17]. The main objective of this analysis is to observe how variations in these parameters impact the resulting changes in the performance of the system and to identify the most influential decision parameters. By performing parameter sensitivity analysis, researchers can determine the optimal values for these parameters that maximize the performance of the helium liquefaction cycle. However, it is important to note that during parameter sensitivity analysis, these decision parameters are commonly optimized separately, which means that the optimal value for each parameter is determined individually. As a result, the combination of these optimal decision parameters may not necessarily produce the highest performance of the system. Therefore, further optimization techniques may be required to identify the combination of decision parameters that produce better performance of the system.

Genetic algorithm has the potential to optimize all the decision parameters simultaneously and is utilized in single-objective optimization studies for the helium liquefaction cycle [18-21]. In these studies, the primary focus lies on system performance, which considers either the liquefaction rate or the cycle's exergy efficiency as objective parameters. The liquefaction rate represents the cooling capacity of the helium cryo-plant to meet the requirement of the cooled object, whereas the higher cycle exergy efficiency is achieved, the less electrical power consumption is required per unit of cooling capacity. However, due to changes in compressor efficiency with pressure ratio [22], optimizing cycle exergy efficiency and liquefaction rate separately may yield significantly different results. Moreover, focusing solely on system performance in single-objective optimization may lead to significant economic costs that may be unacceptable in real projects. Therefore, single-objective optimization is far from meeting the needs of practical engineering requirements.

Non-dominated sorting genetic algorithm-II (NSGA-II) has been widely applied and proven successful in many multi-objective optimization studies [23, 24]. In one study by Chen et al. [25], they considered both cycle exergy efficiency and total annual cost as objective parameters and utilized NSGA-II to obtain an optimal solution that demonstrated superior economic feasibility compared to the results of single-objective optimization for performance, while maintaining a relatively high

system performance. However, it is worth noting that their study did not include an analysis of the stability of the cryogenic system, which is another important factor for real projects. In light of this, Wang et al. [19] conducted research on the stability of expanders, which are the most critical moving parts in helium cryogenic systems. They adopted the stability of expanders as an indicator for the stability of cryogenic systems and investigated the impact of turbine arrangement on the exergy efficiency and stability of these systems using the wheel tip speed of turbine expanders as a stability estimation. However, their analysis did not consider economic cost. Therefore, it is evident that multi-objective optimization offers advantages over single-objective optimization but may still be insufficient to meet practical engineering requirements as additional factors, such as system stability and economic cost, need to be taken into account simultaneously.

According to the review of previous papers in this field, it has been identified that four critical factors need to be considered when optimizing helium liquefaction cycles. Rather than treating all of these factors as objective parameters, it is more appropriate to consider cooling capacity and cycle efficiency as objective parameters, while treating stability and economic cost as constraints. This approach transforms the problem into a constrained multi-objective optimization problem, which can be solved by performing a series of constrained single-objective optimizations. Among the various optimization algorithms available, the interior point method (IPM) has proven to be a highly effective gradient-based optimization algorithm for solving constrained single-objective optimization problems. The IPM optimizes all decision parameters simultaneously during the optimization process. The successful application of the IPM in other thermodynamic systems, such as HVAC systems [26], natural gas liquefaction processes [27, 28], and air separation processes [29], demonstrates its potential for solving the constrained multi-objective optimization problem in helium liquefaction cycles.

In this study, the aim is to obtain an optimal solution for the helium cryo-plant that takes into account both the cooling capacity and cycle efficiency, while ensuring stability and economic feasibility. This will be achieved through the construction of a constrained multi-objective optimization approach. The Collins cycle is chosen as an example of a constrained multi-objective optimization in this study, as it is one of the most representative helium liquefaction cycles. The discharge pressure of the compressor, flow ratio of turbines, and effectiveness of heat exchangers are taken as decision parameters. The liquefaction rate and cycle exergy efficiency, serving as performance indicators, are both selected as objective parameters, rather than cycle exergy efficiency or liquid production rate only. The wheel tip speed of turbines serves as a constraint to ensure the rationality of the optimization results in terms of stability, whereas the UA of heat exchangers serves as another constraint to ensure that the optimization results are reasonable in terms of economic performance. The Pareto frontier which consists of a set of non-dominated solutions is obtained. The TOPSIS method is used as a strategy to select the final optimal solution from the Pareto frontier. Compared to the solution obtained by the single-objective optimization method of liquefaction rate or cycle exergy efficiency, the solution selected by TOPSIS is reasonable in terms of both performance indicators. The wheel tip speed of turbines and UA of heat exchangers of the solutions on the Pareto frontier are studied.

2. Methodology

2.1. System description

Fig. 1 illustrates the schematic of the Collins cycle with LN2 pre-cooling. The system consists of a compressor (Comp) and a cold box. Helium cryo-plants typically use oil-lubricated screw compressors to compress helium gas through a quasi-isothermal process, and it is assumed that the exit temperature of the compressor is at ambient temperature. The cold box is composed of six heat exchangers (HX1-6), two helium turbine expanders (Exp1 and Exp2), one JT valve, and one phase separator. The compressor compresses the high-pressure helium gas, which is then cooled in HX1-HX6 to nearly 7 K. Some of the gas is directed to Exp1 and Exp2 for refrigeration. Following expansion through a J-T valve, the two-phase helium enters the phase separator, where the liquid phase is extracted as the product, while the gaseous phase is recirculated to cool the incoming flow through the heat exchangers before being mixed with the make-up flow. The study has been conducted based on the following assumptions:

1. The system is operating in a steady state.
2. The ambient temperature and pressure are 300 K and 105 kPa. (T_1=300 K)
3. The temperature of helium at the outlet of the hot side in HX1 is 80 K. (T_2=80K).
4. Pressure drop occurs in the low-pressure and high-pressure sides of heat exchangers are 2 kPa and 1 kPa respectively; any heat leak into the system is assumed to be negligible.
5. The mass flow rate through the compressor is kept at 100 g/s, and the suction pressure of the compressor is at 105 kPa; the make-up gaseous helium is at ambient temperature.
6. The isentropic efficiency for turbine expanders (Exp1 and Exp2) is 69% and 66% and does not vary with pressure, temperature, or mass flow rate.

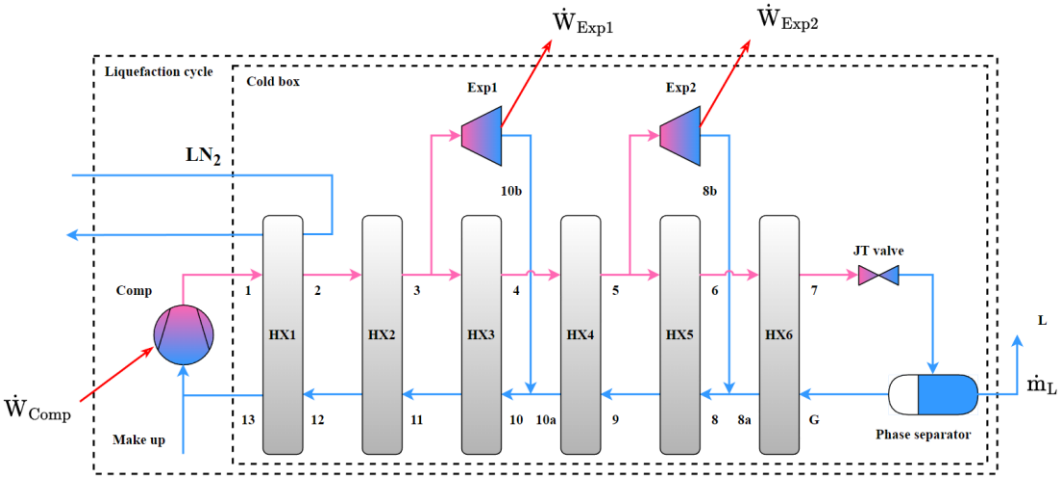

Fig. 1 Schematic of Collins helium liquefaction cycle with LN_2 precooling

Assumption 3, which determines the value of the temperature at the outlet of the hot side in HX1 (T2), is based on engineering practice and is also mentioned in the optimization study of helium liquefaction cycle with LN_2 precooling [19]. Assumption 4, regarding the simplified pressure drops for exchangers, acknowledges that this approach does not fully capture the pressure drop dependency on the heat exchanger's capacity. In addition, it is important to note that the assumption of neglecting heat leak is a common practice for simplifying calculations and is widely adopted in previous literature, as

indicated in references [21, 25]. Assumption 6, concerning the value of the isentropic efficiency for turbine expanders, is set based on the information provided in reference [19]. It is noteworthy that the assumption of constant turbine expander efficiency, regardless of operating conditions, is widely adopted in previous literature, as indicated in references [7, 20].

2.2. Objective parameters

2.2.1 Cycle exergy efficiency

The second law of thermodynamics is the foundation of exergy analysis, which reveals insights into the irreversible losses occurring throughout the entire liquefaction cycle, including specific components. By pinpointing these losses, we can determine the locations of irreversibility and guide the direction of system performance improvements. An exergy balance [30] applied across the control volume of the Collins cycle shown in Fig. 1 results in:

$$\dot{W}_{\mathrm{Comp}} + \dot{E}x_{\mathrm{LN}} + \dot{E}x_{\mathrm{makeup}} = \dot{E}x_{\mathrm{GN}} + \dot{W}_{\mathrm{Exp1}} + \dot{W}_{\mathrm{Exp2}} + \dot{E}x_{\mathrm{L}} + \dot{E}x_{\mathrm{des}} \tag{1}$$

where, $\dot{\mathrm{E}}\mathrm{x}$ refers to the exergy rate, W, $\dot{\mathrm{W}}$ refers to the power consumption or generated power, W. The subscripts “LN”, “GN”, “makeup”, “L”, and “des” correspond to liquid nitrogen, gaseous nitrogen, make-up gas, liquid helium, and exergy destruction respectively. Thus, the three terms on the left-hand side of the equation (1) represent the exergy rate associated with the power consumption of the compressor, liquid nitrogen, and make-up gas, respectively. On the right side of the equation (1), the five terms represent the exergy rate associated with nitrogen gas, output power from turbine expanders, yielded liquid helium, and the exergy destruction rate of the whole system respectively.

The cycle exergy efficiency is defined as the ratio of exergy input to exergy output of the cycle, and it can be utilized to evaluate the efficiency of the helium cryo-plant. In these plants, the power generated by expanders is commonly not recovered, and the evaporated liquid nitrogen is often vented into the atmosphere. Consequently, the available exergy output of the whole system is represented solely by $\dot{E}x_{\mathrm{L}}$. As the make-up gas is nearly at ambient state, its associated exergy rate is almost zero. Additionally, since liquid nitrogen is an inexpensive industrial byproduct and its consumption remains relatively constant when the mass flow rate through the hot side of HX1 is constant, the exergy rate corresponding to liquid nitrogen is not taken into account. Therefore, the exergy input of the system is solely the power consumption of the compressor. As a result, the cycle exergy efficiency can be calculated as follows:

$$\eta_{\mathrm{Ex,cycle}} = \frac{\dot{E}x_{\mathrm{L}}}{\dot{W}_{\mathrm{Comp}}} \tag{2}$$

The $\dot{\mathrm{W}}_{\mathrm{Comp}}$ is defined as the ratio of the exergy rate output of the compressor to isothermal efficiency and can be calculated as:

$$\dot{W}_{\mathrm{Comp}} = \frac{\dot{E}x_{\mathrm{Comp}}}{\eta_{\mathrm{T}}} \tag{3}$$

Practically, the value of η_{T} varies with the compression ratio of the compressor. In this study, the value of η_{T} is calculated using the following equation, which is fitted through the data presented in this book [31]:

$$\eta_T = n_1 + n_2\,pr + n_3\,pr^2 + n_4\,pr^3 + n_5\,pr^4 + n_6\,pr^5 + n_7\,pr^6$$
$$\begin{cases} n_1 = -0.504378,\ n_2 = 1.30627,\ n_3 = -1.18685,\ n_4 = 0.652832 \\ n_5 = -0.190443,\ n_6 = 0.027333,\ n_7 = -0.00152424 \end{cases},\quad pr < 4.32 \qquad (4)$$
$$\begin{cases} n_1 = 0.311803,\ n_2 = 0.0989933,\ n_3 = -0.0163324,\ n_4 = 0.00113159 \\ n_5 = -0.0000413396,\ n_6 = 7.84088E-07,\ n_7 = -6.12810E-09 \end{cases},\ pr \geq 4.32$$

where, *pr* refers to the compression ratio of compressor (p_1/p_{13}), $n_{1\text{-}6}$ refer to the coefficients of the fitting formula.

2.2.2 Liquefaction rate

To effectively maintain a cooled object at liquid helium temperatures, the helium cryo-plant must achieve a specific cooling capacity. The cooling capacity is equal to the rate of helium liquefaction when the mass flow rate through the compressor is sustained at a constant level. Thus, the liquefaction rate emerges as another critical objective parameter that must be taken into account. The approach for determining the liquefaction rate entails solving the thermodynamic model of the Collins cycle, and this value is designated by $\dot{m}_L$ within the specific confines of this study.

2.3. Constraints

2.3.1 Economic cost

Heat exchangers play a pivotal role in helium cryo-plants by recovering the cooling power of low-pressure helium gas after the phase separator, affecting both the liquefaction rate and cycle exergy efficiency. While increasing heat exchange surface area can improve these factors, it may also lead to higher economic costs as a result. With this in mind, in this study, the UA is used as an economic constraint to ensure the optimization results are rational in terms of economic performance. According to LMTD method [32], UA is calculated as:

$$UA = \frac{\dot{Q}}{\Delta T_{\mathrm{LM}}} \qquad (5)$$

where, ΔT_{LM} refers to the log mean temperature difference, and is calculated as:

$$\Delta T_{\mathrm{LM}} = \frac{(T_{\mathrm{hot,out}} - T_{\mathrm{cold,in}}) - (T_{\mathrm{hot,in}} - T_{\mathrm{cold,out}})}{\ln\left(\frac{T_{\mathrm{hot,out}} - T_{\mathrm{cold,in}}}{T_{\mathrm{hot,in}} - T_{\mathrm{cold,out}}}\right)} \qquad (6)$$

Due to the temperature-dependent specific heat capacity of helium within the heat exchanger, it is necessary to subdivide the exchanger into smaller sections to calculate the UA value of each portion accurately, and then add them together to determine the overall UA of the heat exchanger. As a result, the UA of HX2-6 is calculated as:

$$\Delta\dot{Q} = \frac{\dot{Q}}{num}$$

$$\begin{cases} h_{\mathrm{hot},i} = h_{\mathrm{hot,in}} - \dfrac{\Delta\dot{Q}(i-1)}{\dot{m}_{\mathrm{hot}}} \\ T_{\mathrm{hot},i} = Temp(h_{\mathrm{hot},i}, p_{\mathrm{hot}}) \\ h_{\mathrm{cold},i} = h_{\mathrm{cold,out}} - \dfrac{\Delta\dot{Q}(i-1)}{\dot{m}_{\mathrm{cold}}} \\ T_{\mathrm{cold},i} = Temp(h_{\mathrm{cold},i}, p_{\mathrm{cold}}) \end{cases}, \ i = 1, 2, ..., num+1 \tag{7}$$

$$\begin{cases} \Delta T_{\mathrm{LM},i} = \dfrac{(T_{\mathrm{hot},i} - T_{\mathrm{cold},i}) - (T_{\mathrm{hot},i+1} - T_{\mathrm{cold},i+1})}{\ln\left(\dfrac{T_{\mathrm{hot},i} - T_{\mathrm{cold},i}}{T_{\mathrm{hot},i+1} - T_{\mathrm{cold},i+1}}\right)} \\ \Delta UA_i = \dfrac{\Delta\dot{Q}}{\Delta T_{\mathrm{LM},i}} \end{cases}, \ i = 1, 2, ..., num$$

$$UA = \sum_{i=1}^{num} \Delta UA_i$$

where, num refers to the number of sections of a heat exchanger, and *Temp* refers to the program function used to calculate the temperature. Considering the second assumption and the fixed mass flow rate through the compressor, it can be inferred that the working conditions of HX1 almost remain unchanged, resulting in a relatively fixed UA value. Therefore, the UA value of HX1 is not taken into consideration in the study.

2.3.2 Stability

The turbine is regarded as the keystone in terms of both system efficiency and operational stability in helium cryogenics. To achieve maximum isentropic efficiency under design conditions, the turbine must operate at its optimal wheel tip speed. However, as wheel tip speed increases, vibrations and bearing failures are expected to occur more frequently. Hence, the wheel tip speed is selected as the stability constraint to ensure the optimization results are rational in terms of stability. In the study, this quantity is designated by *vel*, m/s. The calculation formula of *vel* is shown as:

$$vel = 0.66\sqrt{2\Delta h_{\mathrm{ideal}}} \tag{8}$$

where, 0.66 is the estimated characteristic ratio obtained from this paper [19], $\Delta h_{\mathrm{ideal}}$ represents the specific enthalpy drop during the ideal expansion process, J/kg.

2.4. Optimization process

Previous studies [7, 8, 19] have conducted parameter sensitivity analyses, which have established that certain parameters have a significant influence on the performance, economic cost, and stability of a cycle. Specifically, when the cycle structure and total mass flow rate through the compressor are fixed, the discharge pressure of the compressor, flow ratio of turbines, and effectiveness of heat exchangers are considered to be the most influential parameters. In the optimization study conducted, these parameters were chosen as decision parameters. This means that during the iterations of the optimization algorithm, the values of these decision parameters were varied within specific ranges. The detailed ranges of these parameter values can be found in Tab. 1.

Tab. 1 Range of values of decision parameters

Decision parameter	Range
Effectiveness of HX1-5	(0.7, 1)
$\dot{m}_{\mathrm{Exp1}}$	(0.1, 0.85)
$\dot{m}_{\mathrm{Exp2}}$	(0.1, 0.85)
Upper limit of $\dot{m}_{\mathrm{Exp1}} + \dot{m}_{\mathrm{Exp2}}$	0.95
pr	(2, 30)

The constrained multi-objective optimization for the Collins cycle is transformed into a sequence of constrained single-objective optimizations given as:

$$\max_{x} \ \eta_{\mathrm{Ex,cycle}} \quad \text{subject to} \begin{cases} vel \leqslant vel_{\max} \\ UA_{\mathrm{tot}} \leqslant UA_{\mathrm{tot,max}} \\ \dot{m}_{\mathrm{L}} \geqslant \dot{m}_{\mathrm{L,lower}} \end{cases} \tag{9}$$

where, the objective only contains $\eta_{\mathrm{Ex,cycle}}$, and the constraints involve *vel*, *UA*, and $\dot{m}_{\mathrm{L}}$. In this context, the value of $vel_{\max}$ is set to 300 m/s based on practical experience. UA_{tot} represents the sum of *UA* of HX2-6. The value of $UA_{\mathrm{tot,max}}$ is determined to be 184582 W/K, obtained through parameter-sensitive analysis [5,6]. It should be noted that the current value of $UA_{\mathrm{tot,max}}$ is given as an example of constrained optimization and can be adjusted as needed. Throughout these constrained single-objective optimizations, $\dot{m}_{\mathrm{L,lower}}$ increases from its minimum to maximum value. The minimum value of $\dot{m}_{\mathrm{L,lower}}$ is obtained by optimizing $\eta_{\mathrm{Ex,cycle}}$ with constraints of $vel_{\max}$ and $UA_{\mathrm{tot,max}}$, while the maximum value of $\dot{m}_{\mathrm{L,lower}}$ is obtained by optimizing $\dot{m}_{\mathrm{L}}$ with constraints of $vel_{\max}$ and $UA_{\mathrm{tot,max}}$. In this paper, forty values were generated by performing an even interpolation between the maximum and minimum values of $\dot{m}_{\mathrm{L,lower}}$.

In this work, the optimization of the Collins cycle utilizes the IPM implemented in MATLAB's built-in NLP solver, fmincon. The IPM approach solves the optimization problem iteratively by finding a new point within the feasible region that is closer to the optimal solution in each iteration. This is achieved by solving a sequence of barrier subproblems, where the objective function, equality constraints, and inequality constraints are modified to incorporate the barrier function. In implementing the IPM, MATLAB's toolbox provides the necessary functions, making the programming process more manageable. The required gradient matrix for the interior point method is determined through automatic differentiation using ADiMat [33]. This approach simplifies the process and enhances the efficiency of the optimization calculations for the Collins cycle.

3. Results and discussions

3.1. Constrained single-objective optimization

Tab. 2 and Tab. 3 present the results of constrained single-objective optimization of $\eta_{\mathrm{Ex,cycle}}$ and $\dot{m}_{\mathrm{L}}$, respectively. It is observed that from Tab. 2 to Tab. 3, there was a decrease in cycle efficiency from 20.9354% to 12.2203%, a decrease of 41.629%. In addition, from Tab. 3 to Tab. 2, there was a decrease in the helium liquefaction rate from 0.1072 kg/s to 0.0773 kg/s, a decrease of 27.892%. Such a significant difference between the results indicates that single-objective optimization may not be

sufficient to meet actual system requirements, highlighting the importance of multi-objective optimization to achieve optimal results that meet all system requirements. Moreover, it is worth noting that the *vel* of Exp1 in Tab. 3 is 300 m/s while the *vel* of Exp1 in Tab. 2 is 284 m/s. This implies that the stability constraint ($vel \leq vel_{max}$) is inactive when the cycle exergy efficiency is the objective parameter. This further emphasizes the difference between the optimization of cycle exergy efficiency and liquefaction rate.

Tab. 2 constrained single-objective optimization of $\eta_{Ex,cycle}$

	HX2	HX3	HX4	HX5	HX6
η_{hx} (%)	98.62	98.62	98.52	98.90	99.48
UA (W/K)	112646	25125	31598	12481	2732
UA_{tot} (W/K)	184582				
	Exp1		Exp2		
$\dot{m}_{Exp}$ (kg/s)	0.467		0.377		
vel (m/s)	284		160		
pr	7.47				
$\eta_{Ex,cycle}$ (%)	20.94				
$\dot{m}_L$ (kg/s)	0.0773				

Tab. 3 constrained single-objective optimization of $\dot{m}_L$

	HX2	HX3	HX4	HX5	HX6
η_{hx} (%)	99.59	99.22	88.98	99.62	99.43
UA (W/K)	133443	18588	4446	20757	7348
UA_{tot} (W/K)	184582				
	Exp1		Exp2		
$\dot{m}_{Exp}$ (kg/s)	0.645		0.147		
vel (m/s)	300		193		
pr	19.99				
$\eta_{Ex,cycle}$ (%)	12.22				
$\dot{m}_L$ (kg/s)	0.107				

The detailed temperature and pressure values resulting from the constrained single-objective optimization of $\eta_{Ex,cycle}$ and $\dot{m}_L$ have been incorporated into the T-s diagram shown in Fig. 2 and Fig. 3, respectively. This allows for a comprehensive examination and verification of the thermodynamic behavior of the system. The conservation of energy is an essential principle in thermodynamics. By examining the mass flow rate values in Tab. 2 and Tab. 3, along with the corresponding thermodynamic values in Fig. 2 and Fig. 3, it is evident that there is no violation of energy conservation in the optimized system. Furthermore, the pinch point temperature difference is a critical parameter for heat exchangers and is directly related to the second law of thermodynamics. The fact that the pinch point temperature differences for all heat exchangers shown in the figures are greater than zero confirms that there is no violation of the second law of thermodynamics in the optimized Collins cycle. This evidence indicates that the optimization process has been successful in achieving a

thermodynamically feasible solution. Therefore, based on these observations, it can be concluded that the thermodynamic calculations performed on the Collins cycle in this study are deemed credible and reliable.

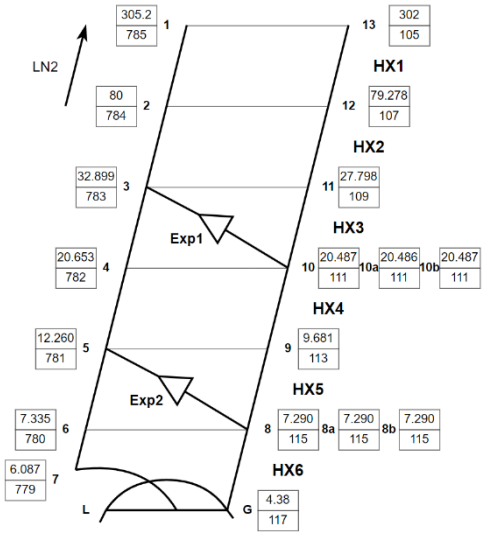

Fig. 2 T-s diagram of constrained single-objective optimization of $\eta_{Ex,cycle}$

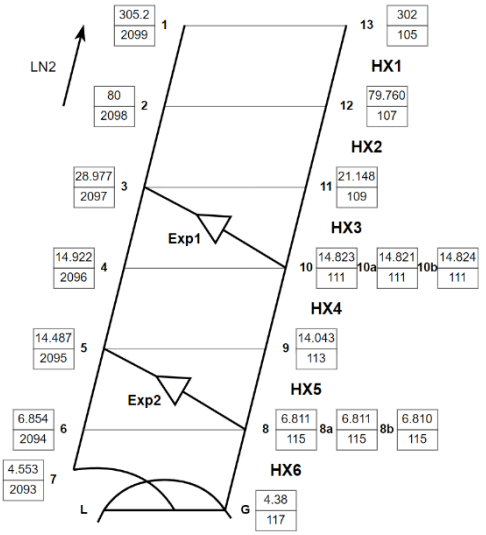

Fig. 3 T-s diagram of constrained single-objective optimization of $\dot{m}_L$

3.2. Constrained multi-objective optimization results

After solving a sequence of optimizations described by Equation (9), we obtained the results of constrained multi-objective optimization of cycle exergy efficiency and liquefaction rate, which are shown in Fig. 4. It is noteworthy that, based on the single-objective optimizations previously described, the maximum and minimum values of liquefaction rate are 0.1072 and 0.0773, respectively. In Fig. 4, the blue dots represent the Pareto frontier of cycle exergy efficiency and liquefaction rate, which is the set of optimal solutions for the constrained multi-objective optimization problem. All solutions on this

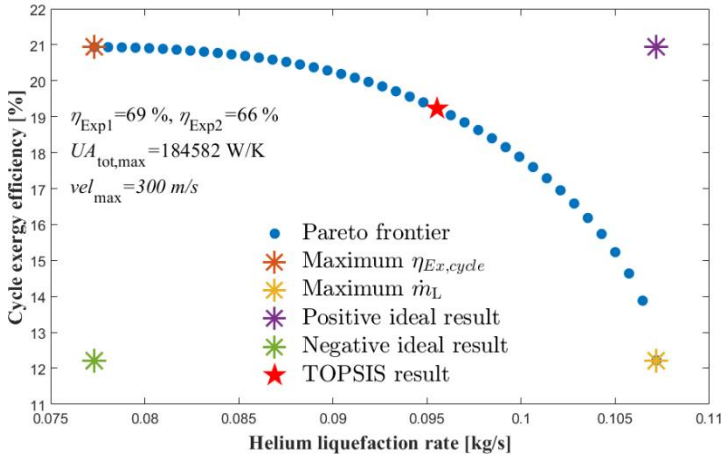

Fig. 4 Pareto frontier of $\eta_{Ex,cycle}$ and $\dot{m}_L$

set are non-dominant. The orange and yellow asterisks located in the upper left and lower right corners, respectively, represent the cases where the cycle exergy efficiency and helium liquefaction rate are at their highest values. The purple asterisk located in the upper right corner represents the positive ideal solution, where both cycle efficiency and helium liquefaction rate reach their maximum values

simultaneously. The green asterisk located in the lower left corner represents the negative ideal solution, where both cycle efficiency and helium liquefaction rate are at their minimum values.

The Technique for Order of Preference by Similarity to Ideal Solution (TOPSIS) method is a commonly used multiple-attribute-decision-making (MADM) method for selecting the final optimal solution from the Pareto frontier, which is utilized in this study. The method calculates the non-dimensional distance between each solution on the Pareto frontier to the positive and negative ideal solutions to select the solution with the highest score based on this distance. The method follows a series of steps, beginning with the nondimensionalization of the values of all solutions in the Pareto frontier according to Equation (10). Subsequently, the scores of these optimal solutions are calculated following Equation (11). Finally, the solution with the highest score is selected as the final and optimal solution.

$$\begin{aligned} \eta^{\mathrm{n}}_{\mathrm{Ex,cycle,i}} &= \frac{\eta_{\mathrm{Ex,cycle},i}}{\sqrt{\sum_{i=1}^{\mathrm{m}} (\eta_{\mathrm{Ex,cycle},i})^2}} \\ \dot{m}^{\mathrm{n}}_{\mathrm{L},i} &= \frac{\dot{m}_{\mathrm{L},i}}{\sqrt{\sum_{i=1}^{\mathrm{m}} (\dot{m}_{\mathrm{L},i})^2}} \end{aligned} \tag{10}$$

where, m represents the number of solutions on the Pareto frontier, subscript *i* represents the index for a certain solution on the Pareto frontier, and superscript n represents nondimensionalization.

$$\begin{aligned} \mathrm{d}^{\mathrm{n}}_{+,i} &= \sqrt{(\eta^{\mathrm{n}}_{\mathrm{Ex,cycle,max}} - \eta^{\mathrm{n}}_{\mathrm{Ex,cycle,i}})^2 + (\dot{m}^{\mathrm{n}}_{\mathrm{L,max}} - \dot{m}^{\mathrm{n}}_{\mathrm{L},i})^2} \\ \mathrm{d}^{\mathrm{n}}_{-,i} &= \sqrt{(\eta^{\mathrm{n}}_{\mathrm{Ex,cycle,min}} - \eta^{\mathrm{n}}_{\mathrm{Ex,cycle,i}})^2 + (\dot{m}^{\mathrm{n}}_{\mathrm{L,min}} - \dot{m}^{\mathrm{n}}_{\mathrm{L},i})^2} \\ \mathrm{S}_i &= \frac{\mathrm{d}^{\mathrm{n}}_{-,i}}{\mathrm{d}^{\mathrm{n}}_{+,i} + \mathrm{d}^{\mathrm{n}}_{-,i}} \end{aligned} \tag{11}$$

Quantities $\mathrm{d}^{\mathrm{n}}_{+}$ and $\mathrm{d}^{\mathrm{n}}_{-}$ respectively represent the nondimensional distance between the i-th optimal solution on the Pareto frontier and the positive and negative ideal solutions, S_i represents the score of the i-th optimal solution on the Pareto frontier. The cycle exergy efficiency of the solution chosen by TOPSIS is 19.23%, which presents a decrease of 8.1623% compared to the maximum value and an increase of 57.333% compared to the minimum value. Moreover, the helium liquefaction rate of the TOPSIS solution amounts to 0.0956 kg/s, representing a decrease of 10.821% compared to the maximum value and an increase of 23.674% compared to the minimum value. Our analysis indicates that the optimal solution selected by TOPSIS effectively balances the two performance indicators of cycle exergy efficiency and helium liquefaction rate.

Fig. 5 displays the wheel tip speeds of Exp1 and Exp2 for each solution on the Pareto frontier of $\dot{m}_{\mathrm{L}}$ and $\eta_{\mathrm{Ex,cycle}}$, represented by round dots. The *vel* of Exp1 shows an increase as $\dot{m}_{\mathrm{L}}$ increases but remains constant after reaching the upper limit value of the stability constraint. Meanwhile, the wheel tip speed of Exp2 exhibits a linear increase with an increase in $\dot{m}_{\mathrm{L}}$ and remains far away from the upper limit of wheel speed. It is evident that the stability constraint is inactive for Exp2 in all solutions on the Pareto frontier, and this can be attributed to the relatively low temperature present at the inlet of Exp2.

Fig. 6 displays the variation of *UA* of HX2-6 for each solution on the Pareto frontier of $\dot{m}_{\mathrm{L}}$ and $\eta_{\mathrm{Ex,cycle}}$. It is evident that turning points exist in the trend of *UA* variation with $\dot{m}_{\mathrm{L}}$ for HX2-4. The *UA* of HX2 initially decreases linearly in response to an increase in $\dot{m}_{\mathrm{L}}$, after which it increases at a

steeper slope. In contrast, the *UA* of HX3 increases linearly with $\dot{m}_L$ initially and subsequently exhibits a linear decrease. The *UA* of HX4 initially decreases linearly with an increase in $\dot{m}_L$ and then decreases at a steeper slope after passing the turning point. Importantly, all turning points occur precisely at the point where the *vel* of Exp1 reaches the upper limit of stability constraint. This finding indicates that the stability constraint has a significant impact on the design of the component parameter of the system, an aspect that has not been considered in previous studies.

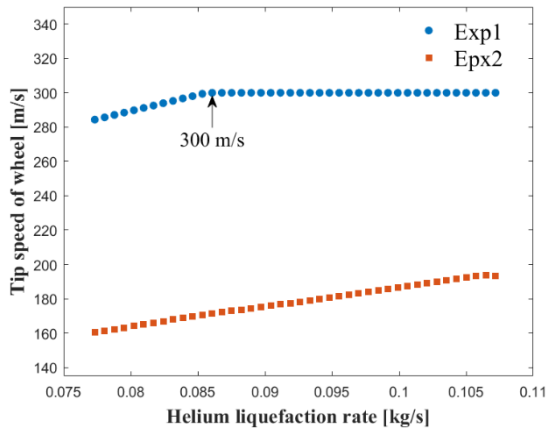

Fig. 5 *vel* corresponding to solutions on the Pareto frontier of $\eta_{Ex,cycle}$ and $\dot{m}_L$

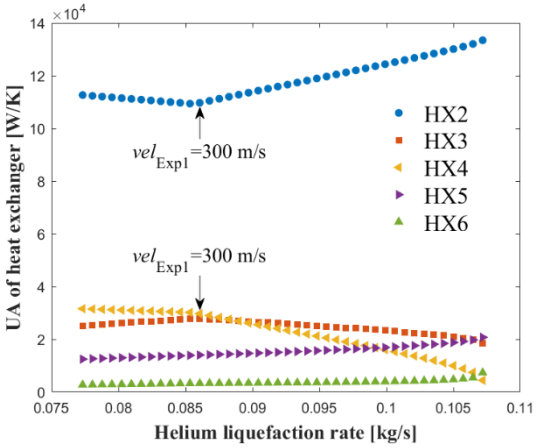

Fig. 6 *UA* corresponding to solutions on the Pareto frontier of $\eta_{Ex,cycle}$ and $\dot{m}_L$

3.3. Analysis of different optimization results

The impact of constraints on the helium liquefaction cycle was assessed through several optimization calculations, and the results are summarized in Tab. 4. In the first set of calculations (No.1 - No.3), the focus was on the single-objective optimization of liquefaction rate. No.1 represented the optimization without any constraints, while No.2 represented the optimization with a constraint on UA_{tot}, and No.3 represented the optimization with constraints on both UA_{tot} and *vel*. In the second set of calculations (No.4 - No.6), the focus was on the single-objective optimization of cycle efficiency. No.4 represented the optimization without any constraints, while No.5 represented the optimization with a constraint on UA_{tot}, and No.6 represented the optimization with constraints on both UA_{tot} and *vel*. In the third set of calculations (No.7 - No.9), the focus was on the multi-objective optimization of liquefaction rate and cycle efficiency using TOPSIS method. No.7 represented the optimization without any constraints, while No.8 represented the optimization with a constraint on UA_{tot}, and No.9 represented the optimization with constraints on both UA_{tot} and *vel*. The values for these constraints were 184,582 W/K for UA_{tot} and 300 m/s for *vel*.

From No.1 to No.2, when UA_{tot} is constrained, there is a decrease in UA from 341911 W/K to 184582 W/K, a decrease of 46.01%. This constraint also results in a decrease in liquefaction rate from 0.128 kg/s to 0.123 kg/s, a decrease of 3.91%. Compared to the significant decrease in UA, the decrease in liquefaction rate is minimal. Similar observations were made when comparing No.4 to No.5 and No.7 to No.8. These findings emphasize the importance of considering constraints on UA_{tot} during optimization to achieve a balance between performance and cost. Without UA_{tot} constraints, there is a significant increase in the area of heat exchangers, leading to increased costs without substantial performance benefits.

Additionally, when *vel* is not constrained, the operation of turbines could become unstable, as evidenced by the values of 409 m/s and 363 m/s in No.1 and No.2. However, when the constraint on *vel* was introduced (No.3), the velocity of the first turbine was reduced to 300 m/s, which led to a decrease in the liquefaction rate. Similar observations were made for the multi-objective optimization calculations (No.7, No.8, and No.9). These findings suggest that while a high-performance helium liquefaction cycle may seem desirable, it may not be practical if the operation of turbines becomes unstable without constraints on *vel*. Therefore, considering constraints on both UA_{tot} and *vel* is essential in optimizing the helium liquefaction cycle.

Tab. 4 Results of different optimization

Optimization No.	Objective parameter(s)	Constraint(s)	$\dot{m}_L$ (kg/s)	$\eta_{Ex,cycle}$ (%)	UA_{tot} (W/K)	vel_{Exp1} (m/s)	vel_{Exp1} (m/s)
1	$\dot{m}_L$	none	0.128	11.16	341911	409	248
2	$\dot{m}_L$	UA_{tot}	0.123	11.18	184582	363	199
3	$\dot{m}_L$	UA_{tot} and *vel*	0.107	12.22	184582	300	193
4	$\eta_{Ex,cycle}$	none	0.0769	22.73	431780	283	155
5	$\eta_{Ex,cycle}$	UA_{tot}	0.0773	20.94	184582	284	160
6	$\eta_{Ex,cycle}$	UA_{tot} and *vel*	0.0773	20.94	184582	284	160
7	$\dot{m}_L$ and $\eta_{Ex,cycle}$	none	0.104	19.93	396188	339	194
8	$\dot{m}_L$ and $\eta_{Ex,cycle}$	UA_{tot}	0.102	18.52	184582	332	193
9	$\dot{m}_L$ and $\eta_{Ex,cycle}$	UA_{tot} and *vel*	0.0955	19.23	184582	300	181

4. Conclusion

In this work, a constrained multi-objective optimization using the interior point method is conducted to balance the liquefaction rate and cycle exergy efficiency of helium cryo-plants, while also ensuring stability and economic feasibility. By employing this approach, the Pareto frontier of the two objectives, $\eta_{Ex,cycle}$ and $\dot{m}_L$, is obtained. The Technique for Order of Preference by Similarity to Ideal Solution (TOPSIS), which is one of the Multiple Attribute Decision Making (MADM) methods, is then utilized to select the final optimal solution from the calculated Pareto frontier. Compared to the constrained optimization of $\eta_{Ex,cycle}$, the TOPSIS result increases the $\dot{m}_L$ by 23.674%, at the cost of an 8.162% reduction in $\eta_{Ex,cycle}$. Similarly, compared to the constrained optimization of $\dot{m}_L$, the TOPSIS result increases the $\eta_{Ex,cycle}$ by 57.333%, but a 10.821% reduction in $\dot{m}_L$ is observed. These conclusions indicate that the constraint multi-objective optimization of liquefaction rate and cycle exergy efficiency is more practical than optimizing only one of them. Furthermore, analysis of wheel tip speed on the Pareto frontier reveals that the constraint on wheel tip speed is inactive for turbines operating at low temperatures. Additionally, the constraint on wheel tip speed has a significant impact on the distribution of UA_{tot} of heat exchangers. By comparing the results of optimization calculations with and without constraints, the significance of considering constraints on UA_{tot} and *vel* in the optimization of the Collins cycle becomes evident. Neglecting these constraints can lead to increased costs without substantial performance benefits, as well as potential turbine instability. Therefore, it is crucial to incorporate these constraints to achieve a balance between performance and cost in the helium liquefaction cycle optimization. This approach allows for the design of helium cryo-plants by

simultaneously considering cooling capacity, cycle exergy efficiency, economic cost, and stability. It is important to note that the consideration of economic indicators in this article is described as simplistic, and future work will aim to provide a more detailed analysis in this regard.

Acknowledgment

The authors gratefully acknowledge the support from Hefei Comprehensive National Science Center and the High Magnetic Field Laboratory of Anhui Province.

Nomenclature

d_{+}^{n} - nondimensionalized distance between a solution and the positive ideal solution	n_{1-7} - Coefficients of the fitting formula for isothermal efficiency calculation
d_{-}^{n} - nondimensionalized distance between a solution and the negative ideal solution	$\dot{Q}$ - heat transfer rate, [W]
Δh_{ideal} - specific enthalpy drop during the ideal expansion process, [J/kg]	*UA* - the product of overall heat transfer coefficient and heat exchange area, [W/K]
$\dot{E}x$ - exergy rate, [W]	*vel* - Wheel tip speed of turbines, [m/s]
$\dot{m}$ - mass flow rate, [kg/s]	$\dot{W}$ - power consumption or produced work, [W]
Greek symbols	
η - efficiency or effectiveness	
Subscripts	
Cold - cold side of heat exchanger	L - liquid helium
des - exergy destruction	LM - logarithmic mean
ex - exergy	LN - liquid nitrogen
GN - gaseous nitrogen	makeup - makeup gaseous helium
hot - hot side of heat exchanger	max - maximum
hx - heat exchanger	min - minimum
i - index for each solution on the Pareto frontier	out - outlet
in - inlet	T - related to the isothermal process

References

[1] Howell, M., *et al.*, Cryogenic Control System Operational Experience At SNS, *EPJ techniques and instrumentation, 8* (2021), 4

[2] Mastracci, B., *et al.*, Commissioning of A Replacement Subatmospheric Cold Box for Jefferson Lab's Central Helium Liquefier, *IOP Conference Series: Materials Science and Engineering, 1240* (2022), 012069

[3] Casagrande, F., *et al.*, FRIB cryogenic system status, *Proceedings*, IOP Conference Series: Materials Science and Engineering, March 2020, Vol. 755, pp. 012089

[4] Bai, H., *et al.*, Cryogenics In EAST, *Fusion Engineering and Design*, *81* (2006), 23, pp. 2597-2603

[5] Kalinin, V., *et al.*, ITER Cryogenic System, *Fusion Engineering and Design*, *81* (2006), 23, pp. 2589-2595

[6] Ferlin, G., *et al.*, 5-year operation experience with the 1.8 K refrigeration units of the LHC cryogenic system, *Proceedings*, IOP Conference Series: Materials Science and Engineering, 2015, Vol. 101, pp. 012141

[7] Thomas, R. J., *et al.*, Role of Expanders in Helium Liquefaction Cycles: Parametric Studies Using Collins Cycle, *Fusion Engineering and Design*, *86* (2011), 4-5, pp. 318-324

[8] Thomas, R. J., *et al.*, Role of Heat Exchangers in Helium Liquefaction Cycles: Simulation Studies Using Collins Cycle, *Fusion Engineering and Design*, *87* (2012), 1, pp. 39-46

[9] Thomas, R. J., *et al.*, Exergy Based Analysis on Different Expander Arrangements in Helium Liquefiers, *International Journal of Refrigeration*, *35* (2012), 4, pp. 1188-1199

[10] Thomas, R. J., *et al.*, Exergy Analysis of Helium Liquefaction Systems Based on Modified Claude Cycle with Two-Expanders, *Cryogenics*, *51* (2011), 6, pp. 287-294

[11] Thomas, R. J., *et al.*, Application of Exergy Analysis in Designing Helium Liquefiers, *Energy*, *37* (2012), 1, pp. 207-219

[12] Thomas, R. J., *et al.*, Optimum Number of Stages and Intermediate Pressure Level for Highest Exergy Efficiency in Large Helium Liquefiers, *International Journal of Refrigeration*, *36* (2013), 8, pp. 2438-2457

[13] Lei, G., *et al.*, A Novel Intercooled Series Expansion Refrigeration/Liquefaction Cycle Using Pinch Technology, *Applied Thermal Engineering*, *163* (2019), pp. 114336

[14] Larijani, M., *et al.*, Investigation of Effective Parameters on The Performance Of The Helium Liquefaction Cycle, *IJHT*, *37* (2019), 4, pp. 1009-1018

[15] Kundu, A., *et al.*, Exergy Analysis to Determine Appropriate Design and Operating Parameters for Collins Refrigerator-Liquefier Under Mixed Mode Operation, *Refrigeration Science and Technology*, *2012* (2012), pp. 233-239

[16] Kundu, A., Chowdhury, K., Evaluating Performance of Mixed Mode Multistage Helium Plants For Design and Off-Design Conditions By Exergy Analysis, *International Journal of Refrigeration*, *38* (2014), pp. 46-57

[17] Maiti, T. K., *et al.*, Evaluation of An Existing Helium Liquefier in Refrigerator and Mixed-Mode Operation Through Exergy Analysis, *Cryogenics*, *103* (2019), pp. 102977

[18] Cammarata, G., *et al.*, Optimization of a Liquefaction Plant Using Genetic Algorithms, *Applied Energy*, *68* (2001), 1, pp. 19-29

[19] Wang, H. R., *et al.*, The Optimization on Flow Scheme of Helium Liquefier with Genetic Algorithm, *Cryogenics*, *81* (2017), pp. 93-99

[20] Mahmoudabadbozchelou, M., *et al.*, An Economic Approach to Study and Optimize Helium Liquefier, *Cryogenics*, *110* (2020), pp. 103147

[21] Xue, R., *et al.*, Influence of Key Parameters on The Performance of a Helium Cryogenic System in Refrigeration and Liquefaction Modes, *Cryogenics*, *121* (2022), pp. 103386

[22] Ganni, V., *et al.*, Screw Compressor Characteristics for Helium Refrigeration Systems, *Proceedings*, AIP Conference Proceedings, Chattanooga (Tennessee), 2008, Vol. 985, pp. 309-315

[23] Jiang, M., Pan, Z., Optimization of Open Micro-Channel Heat Sink with Pin Fins by Multi-Objective Genetic Algorithm, *Therm. Sci.*, *26* (2022), 4B, pp. 3653-3665

[24] Abdi, H., *et al.*, Multi-Objective Optimization of Operating Parameters of a Pemfc Under Flooding Conditions Using the Non-Dominated Sorting Genetic Algorithm, *Therm. Sci.*, *23* (2019), 6, pp. 3525-3537

[25] Chen, S., *et al.*, Multi-Objective Thermo-Economic Optimization of Collins Cycle, *Energy*, *239* (2022), pp. 122269

[26] Kusiak, A., *et al.*, Minimization of Energy Consumption in HVAC Systems with Data-Driven Models and An Interior-Point Method, *Energy Conv. Manag.*, *85* (2014), pp. 146-153

[27] Watson, H. A. J., *et al.*, Optimization of Single Mixed-Refrigerant Natural Gas Liquefaction Processes Described by Nondifferentiable Models, *Energy*, *150* (2018), pp. 860-876

[28] Jacobsen, M.G., Skogestad, S., Active Constraint Regions for A Natural Gas Liquefaction Process, *Journal of Natural Gas Science and Engineering*, *10* (2013), pp. 8-13

[29] Zhu, Y., *et al.*, Optimal Design of Cryogenic Air Separation Columns Under Uncertainty, *Comput. Chem. Eng.*, *34* (2010), 9, pp. 1377-1384

[30] Sanford, K., Gregory, N., *Thermodynamics*, Cambridge University Press, Cambridge, 2011

[31] Baguer, G. G., The Compression Machines, in: *Cryogenic Helium Refrigeration for Middle and Large Powers*, Springer Nature, 2020, pp. 197

[32] Nellis, G., Klein, S. A., *Heat Transfer*, Cambridge University Press, Cambridge, 2008

[33] Bischof, C. H., *et al.*, Combining source transformation and operator overloading techniques to compute derivatives for MATLAB programs, *Proceedings*, Second IEEE International Workshop on Source Code Analysis and Manipulation Proceedings, October 2002, pp. 65-72

Received: 26.06.2023.
Revised: 30.09.2023.
Accepted: 24.10.2023.